Medicinal Chemistry Research
https://doi.org/10.1007/s00044-019-02492-5

MEDICINAL CHEMISTRY RESEARCH

ORIGINAL RESEARCH



# Synthesis, in vitro antigiardial activity, SAR analysis and docking study of substituted chalcones

David Cáceres-Castillo[1] · Rubén M. Carballo[1] · Ramiro Quijano-Quiñones[1] · Gumersindo Mirón-López[1] · Manlio Graniel-Sabido[1] · Rosa E. Moo-Puc[2] · Gonzalo J. Mena-Rejón[1]

Received: 2 October 2019 / Accepted: 11 December 2019


## Abstract

A series of 15 chalcones-bearing substituents at positions 2, 4, and 5 of rings A and B were synthesized using microwave-assisted Claissen–Smichdt condensation and evaluated for their activity against *Giardia lamblia* and Green monkey kidney cells. Five compounds exhibited activity against *G. lamblia* at $IC_{50}$'s <5 μM. The chalcone **3m** exhibited the highest antigiardial activity ($IC_{50} = 1.03$ μM), even more than the positive control (metronidazole, $IC_{50} = 1.4$ μM), and selectivity (SI = 38.9). A preliminary SAR study suggested that electrophylicity has not relationship with antigiardiasic activity, and the docking study reveals that synthesized chalcones bind at zone 3 of colchicine site, therefore presumably the action mechanism of the synthesized chalcones does not follow the Michael acceptor mechanism.

**Keywords** Synthesis · Substituted chalcones · Antigiardial activity · SAR analysis · Docking study

## Introduction

The flagellated and amitochondriate protozoan *Giardia lamblia* (syn. *G. intestinalis*, *G. duodenalis*) is a human enteric pathogen with the high morbidity worldwide. In 1998, WHO estimated that one billion people living in developing countries was infected by this parasite, and ~280 million cases occurring annually. (Upcroft and Upcroft 2001). Two years later, giardiasis was referred as a ree-merging infectious disease, (Thompson 2000), and in September 2004, it was included in the 'WHO Neglected Diseases Initiative'. (Savioli et al. 2006). More recently, during 2010, 183 million cases of diarrheal disease worldwide associated to *G. lamblia* infection were detected applying the Child Health Epidemiology Reference Group (CHERG) approach (Pires et al. 2015).

The infection by *G. lamblia* occurs when people ingest water or food contaminated with cysts, or through person-to-person contact, or by contact with contaminated fomites. Signs of giardiasis vary between individuals and range from acute or chronic diarrhea to total latency. Clinical symptoms normally begin 1–3 weeks following transmission and may include nausea, vomiting, weight loss, abdominal pain, bloating, and diarrhea (Escobedo et al. 2010). The impact of giardiasis is stronger on undernourished or immunodeficient individuals and on young children (Ankarklev et al. 2010). In 1–5 years old children the infection by *Giardia* can cause failure to thrive syndrome, and delays in the physical growth and cognitive-intellectual development (Halliez and Buret 2013).

The most common drugs used in the treatment of giardiasis are 5-nitroimidazoles (metronidazole, tinidazole, secnidazole, and ornidazole) of which metronidazole being the first-choice option. Notwithstanding, it has been reported heavy side effects of metronidazole such as headache, vertigo, nausea, allergic reactions, and in some cases neurotoxicity, teratogenic, and mutagenic effects. Moreover, resistance can occur in up to 20% of clinical cases (Pasupuleti et al. 2014). This panorama makes necessary to

**Supplementary information** The online version of this article (https://doi.org/10.1007/s00044-019-02492-5) contains supplementary material, which is available to authorized users.

✉ Gonzalo J. Mena-Rejón
mrejon@uady.mx

[1] Facultad de Química, Universidad Autónoma de Yucatán, C. 43 No. 613, Col. Inalámbrica, Mérida 97069 Yucatán, Mexico

[2] Unidad de Investigación Médica Yucatán, Unidad Médica de Alta Especialidad, Centro Médico "Ignacio García Téllez", IMSS, C. 41, No. 439, Col. Industrial, C.P., Mérida 97150 Yucatán, Mexico

Published online: 27 December 2019

maintain a continuous searching for novel antigiardial drug candidates, and natural product are promising scaffolds for such compounds.

The 1,3-diaryl-2-propen-1-one (chalcone) is a common scaffold found in many natural products derived from plants which possess a wide spectrum of interesting biological activities. Also, chalcone derivatives exhibit high bioavailability and tolerance in the organism of mammals (Gaonkar and Vignesh 2017). Advantageously, the α, β-unsaturated ketone moiety is easily synthesizable and chalcones are generally prepared with good yields by condensation reactions via base or acid catalysis (Claisen−Schmidt condensation). For these reasons, many chalcone derivatives have been synthesized, and a high percentage of them have resulted in biologically active compounds with clinical potential against various diseases (Gomes et al. 2017). Noteworthy, the importance of chalcone scaffold in medicinal chemistry has been increasing due to the new evidence supporting it as a privileged structure (Zhuang et al. 2017).

Chalcone-based compounds have maintained the interest of academia and industry across the 20th century due to their wide-ranging biological activities, especially the anti-infective ones (Sahu et al. 2012). Diverse chalcones derivatives have been synthesized for 25 years to evaluate their antimalarial and antileishmanial activities (Gomes et al. 2017; Zhuang et al. 2017). Besides, during the last decade, a series of 25 variously substituted nonnatural chalcones were synthesized to be tested for antigiardial activity. Although only three compounds showed significant antigiardial activity (Fig. 1), the obtained results revealed the importance of oxygenated and nonbulky substituents at *para*-position in chalcone's ring A with for such activity (Montes-Avila et al. 2009).

As a part of our search into antiprotozoal compounds, we synthesized a small library of chalcones derivatives and the activity against *G. lamblia* of the resulting compounds was evaluated together their calculated LogP and electrophilicity indexes in a preliminary structure-antigiardiasic activity (SAR) analysis. Finally, a docking study was performed with the four most active chalcones.

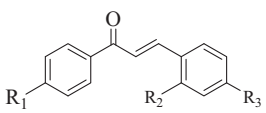


| | $R_1$ | $R_2$ | $R_3$ |
|---|---|---|---|
| $C_1$ | MeO | F | H |
| $C_2$ | MeO | H | Cl |
| $C_3$ | F | H | Me |

**Fig. 1** Reported antigiardiasic chalcones

## Materials and methods

### Chemistry

All commercial reagents were obtained from Sigma-Aldrich (Saint Louis, MO, USA) and used as received. Microwave reactions were conducted in 25 mL open glass vessels using a CEM Discover microwave reactor. Analytical and preparative thin-layer chromatography (TLC) were performed on 25 µm particle size silica gel GF-254 aluminium and glass plates, respectively. Column chromatography was undertaken with 0.063–0.037 mm particle size silica gel. Melting points were determined on an Electrothermal IA9100 apparatus in open capillaries. Fourier transform infrared analysis was performed with a Nicolet iS5 spectrometer in the range of 4000–600 $cm^{-1}$ with 32 scans recorded at 4 $cm^{-1}$ of resolution. $^{1}$H-NMR and $^{13}$C-NMR spectra were recorded in DMSO-d6 on Bruker Avance 400 spectrometer at 400 and 100 MHz, respectively, and the residual solvent peak was used as an internal reference. The $\delta$ values are given in ppm. The low and high-resolution mass spectra were recorded with a Jeol GCmate II mass spectrometer by using electron impact mode at 70 eV.

### General procedure for the preparation of chalcones (3a–o)

An appropriate acetophenone (3.7 mmol) (**1a–e**) and the corresponding benzaldehyde (3.7 mmol) (**2a–c**) were dissolved in EtOH (10 mL), and then 2.2 mL of a 50% NaOH aqueous solution were added dropwise. The resulting reaction mixture was subjected to MW irradiation at 80 °C (70 W) from 2 to 4 h. After time completion, the reaction mixture was poured on 20 mL of chilly water and acidified with 10% HCl aqueous solution until pH 2. The crude products were purified by crystallization or, in a few cases, by silica gel chromatography.

### (*E*)-3-(2-hydroxyphenyl)-1-(4-methylphenyl)-2-propen-1-one (3a)

Pale-yellow powder, crystallized from EtOH-$H_2O$ (1:4), Yield 49%, mp 148–149 °C. IR (KBr) $\nu_{max}$ in $cm^{-1}$: 3240 (OH), 1645 (C=O), 1604 (C=C). $^{1}$H NMR (400 MHz, DMSO-$d_6$): $\delta = 10.3$ (1H, s, C-2′-OH), 8.05 (1H, d, $J =$ 15.8 Hz, H-3), 8.01 (2H, d, $J = 8.0$ Hz, H-2′,H-6′), 7.86 (1H, m, H-3″), 7.85 (1H, d, $J = 15.8$ Hz, H-2), 7.36 (2H, d, $J = 8.4$ Hz, H-3′, H-5′), 7.27 (1H, t, $J = 8.4$ Hz, H-5″), 6.95 (1H, d, $J = 8.0$ Hz, H-6″), 6.87 (1H, t, $J = 7.6$ Hz, H-4″), 2.38 (3H, s, C-4′-Me). $^{13}$C NMR (100 MHz, DMSO-$d_6$): $\delta = 188.9$ (C, C-1), 157.2 (C, C-2″), 143.3 (C, C-4′), 139.2 (CH, C-3), 135.4 (C, C-1′), 132.0 (CH, C-5″), 129.4 (2CH,

C-3′, C-5′), 128.7 (CH, C-3″), 128.5 (2CH, C-2′, C-6′), 121.5 (C, C-1″), 121.0 (CH, C-2), 119.5 (CH, C-4″), 116.3 (CH, C-6″), 21.2 ($CH_3$, C-4′-Me). HRMS (EI+, 70 eV) *m/z*: 238.0990 for $C_{16}H_{14}O_2$ (calcd. 238.0994).

### (*E*)-3-(4-methoxyphenyl)-1-(4-methylphenyl)-2-propen-1-one (3b)

Pale-yellow powder, crystallized from EtOH-$H_2O$ (2:3), Yield 71%, mp 103–104 °C. IR (KBr) $\nu_{max}$ in $cm^{-1}$: 2967 ($CH_3$), 1656 (C=O), 1605 (C=C). $^1H$ NMR (400 MHz, DMSO-$d_6$): $\delta = 8.04$ (d, 2H, $J = 8.0$ Hz, H-2′, H-6′), 7.84 (d, 2H, $J = 8.0$ Hz, H-2″, H-6″), 7.78 (d, 1H, $J = 16$ Hz, H-3), 7.69 (d, 1H, $J = 16$ Hz, H-2), 7.36 (d, 2H, $J = 8.0$ Hz, H-3″, H-5″), 7.01 (d, 2H, $J = 8.0$ Hz, H-3′, H-5′), 3.82 (s, 3H, C-4″-OMe), 2.40 (s, 3H, C-4′-Me) ppm. $^{13}C$ NMR (100 MHz, DMSO-$d_6$): δ 189.0 (C, C-1), 161.8 (C, C-4″), 144.1 (C, C-4′), 143.8 (CH, C-3), 135.8 (C, C-1′), 131.2 (2CH, C-2″, C-6″), 129.8 (C, C-1″), 129.0 (2CH, C-3′, C-5′), 127.8 (2CH, C-2′, C-6′), 120.0 (CH, C-2), 114.9 (2CH, C-3″, C-5″), 55.8 ($CH_3$, C-4″-OMe), 21.6 ($CH_3$, C-4′-Me). HRMS (EI+, 70 eV) *m/z*: 252.3194 $C_{17}$ $H_{16}$ $O_2$ (calcd. 252.3198).

### (*E*)-3-(4-chloro-2-hydroxyphenyl)-1-(4-methylphenyl)-2-propen-1- one (3c)

Orange powder, crystallized from EtOH-$H_2O$ (3:7), Yield 66%, mp 135–136 °C. IR (KBr) $\nu_{max}$ in $cm^{-1}$: 3226 (OH), 1651 (C=O), 1607 (C=C), 745 (C–Cl). $^1H$ NMR (400 MHz, DMSO-$d_6$): $\delta = 10.6$ (brs, 1H, C-2″-OH), 8.03 (m, 3H, H-2′, H-6′, H-6″), 7.98 (d, 1H, $J = 16.0$ Hz, H-3), 7.92 (d, 1H, $J = 16$ Hz, H-2), 7.35 (d, 2H, $J = 7.8$ Hz, H-3′), 7.28 (dd, 1H, $J = 6.8$ and 1.8 Hz, H-4″), 6.94 (d, 1H, $J = 8.7$, H-3″), 2.38 (s, 3H, C-4′-Me). $^{13}C$ NMR (100 MHz, DMSO-$d_6$): $\delta = 188.8$ (C, C-1), 159.0 (C, C-2), 143.7 (C, C-4′), 137.4 (CH, C-3), 135.2 (CH, C-4″), 131.5 (C, C-1′), 129.5 (2CH, C-3′, C-5′), 128.9 (2CH, C-2′, C-6′), 127.5 (CH, C-6″), 123.4 (CH, C-2), 123.3 (C, C-5″), 122.1 (C, C-1″), 118.0 (CH, C-3″), 21.3 ($CH_3$, C-4′-Me). HRMS (EI+, 70 eV) *m/z*: 272.0606 for $C_{16}H_{13}O_2Cl$ (calcd. 272.0604); 274.0616 for $C_{16}H_{13}O_2{}^{37}Cl$ (calcd. 274.0575).

### (*E*)-3-(2-hydroxy-phenyl)-1-(4-methoxy-phenyl)-2-propen-1-one (3d)

Yellow powder, purified by column chromatography (silica gel 74–37 µm, eluent hexane:ethyl acetate gradient), Yield 43%, mp 146–147 °C. IR (KBr) $\nu_{max}$ in $cm^{-1}$: 3287 (OH), 2932 ($CH_3$), 1645 (C=O), 1602 (C=C). $^1H$ NMR (400 MHz, DMSO-$d_6$): $\delta = 10.3$ (brs, 1H, C-2″-OH), 8.11 (d, 2H, $J =$ 7.7 Hz, H-2′, H-6′), 8.04 (d, 1H, $J = 15.7$ Hz, H-3), 7.85 (d, 1H, $J = 15.7$ Hz, H-2), 7.84 (dd, 1H, $J = 7.9$ & 3.9 Hz, H-3″), 7.26 (t, 1H, $J = 7.9$ Hz, H-5″), 7.06 (d, 2H, $J = 7.5$ Hz, H-3′), 6.94 (d, 1H, $J = 8.2$, H-6″), 6.87 (t, 1H, $J = 7.5$ Hz, H-4″), 3.85 (s, 3H, C-4′-OMe). $^{13}C$ NMR (100 MHz, DMSO-$d_6$): $\delta = 188.1$ (C, C-1), 163.5 (C, C-2″), 157.6 (C, C-4′), 139.1 (CH, C-3), 132.3 (C, C-1′), 131.2 (2CH, C-2′, C-6′), 131.1 (CH, C-5″), 129.0 (CH, C-3″), 122.0 (C, C-1″), 121.2 (CH, C-2), 119.9 (CH, C-4″), 116.6 (CH, C-6″), 114.4 (2CH, C-3′), 55.9 ($CH_3$, C-4′-OMe). HRMS (EI+, 70 eV) *m/z*: 254.0949 for $C_{16}H_{14}O_3$ (calcd. 254.0949).

### (*E*)-1,3-bis-(4-methoxy-phenyl)-2-propen-1-one (3e)

Yellow powder, purified by column chromatography (silica gel 74–37 µm, eluent hexane:ethyl acetate gradient), Yield 44%, mp 95–96 °C. IR (KBr) $\nu_{max}$ in $cm^{-1}$: 2962 ($CH_3$), 1655 (C=O), 1601 (C=C). $^1H$ NMR (400 MHz, DMSO-$d_6$): $\delta$ 8.15 (2H, d, $J = 8.8$ Hz, H-2′, H-6′), 7.85 (2H, d, $J =$ 8.8 Hz, H-2″, H-6″), 7.8 (1H, d, $J = 15.6$ Hz, H-3), 7.68 (1H, d, $J = 15.6$ Hz, H-2), 7.08 (2H, d, $J = 8.8$ Hz, H-3′, H-5′), 7.02 (2H, d, $J = 8.8$ Hz, H-3″, H-5″), 3.86 (3H, s, C-4′-OMe), 3.82 (3H, s, C-4″-OMe). $^{13}C$ NMR (100 MHz, DMSO-$d_6$): $\delta = 187.3$ (C, C-1), 163.1 (C, C-4′), 161.2 (C, C-4″), 143.2 (CH, C-2), 130.8 (2CH, C-2′, C-6′), 130.7 (2CH, C-2″, C-6″), 130.7 (C, C-1′), 127.5 (C, C-1″), 119.5 (CH, C-3), 114.4 (2CH, C-2″, C-6″), 114.0 (2CH, C-3′, C-5′), 55.6 ($CH_3$, C-4′-OMe), 55.4 ($CH_3$, C-4″-OMe). HRMS (EI+, 70 eV) *m/z*: 268.1104 for $C_{17}H_{16}O_3$ (calcd. 268.1100).

### (*E*)-3-(5-Chloro-2-hydroxyphenyl)-1-(4-methoxyphenyl)-2-propen-1-one (3f)

Yellow-orange powder, crystallized from EtOH-$H_2O$ (1:4), Yield 61%, mp 150–151 °C. IR (KBr) $\nu_{max}$ in $cm^{-1}$: 3405 (OH), 1646 (C=O), 1601 (C=C), 756 (C-Cl). $^1H$ NMR (400 MHz, DMSO-$d_6$): $\delta = 8.08$ (d, 2H, $J = 8$ Hz, H-2′, H-6′), 8.00 (d, 1H, $J = 16$ Hz, H-3), 7.90 (d, 1H, $J = 16$ Hz, H-2), 7.62 (d, 1H, H-6″), 7.05 (d, 2H, $J = 9.2$ Hz, H-3′, H-5′), 7.02 (dd, 1H, $J = 2.4$ & 8.8 Hz, H-4″), 6.61 (d, 1H, $J =$ 8 Hz, H-3″), 3.85 (s, 3H). $^{13}C$ NMR (100 MHz, DMSO-$d_6$): $\delta = 188.4$ (C, C-1), 164.9 (C, C-2″), 163.2 (C, C-4′), 141.1 (CH, C-3), 131.7 (C, C-1′), 131.6 (2CH, C-2′, C-6′), 131.0 (CH, C-4″), 128.6 (CH, C-6″), 123.8 (C, C-1″), 120.8 (C, C-5″), 119.1 (CH, C-2), 117.9 (CH, C-3″), 114.3 (2CH, C-3′, C-5′), 55.9 ($CH_3$, C-4′-OMe). HRMS (EI+, 70 eV) *m/z*: 288.0562 for $C_{16}H_{13}O_3Cl$ (calcd. 288.0553); 290.0543 for $C_{16}H_{13}O_3{}^{37}Cl$ (calcd. 290.0524).

### (*E*)-3-(2-hydroxy-phenyl)-1-(4-hydroxy-phenyl)-2-propen-1-one (3g)

Yellow powder, crystallized from EtOH-$H_2O$ (2:3), Yield 45%, mp 147–148 °C. IR (KBr) $\nu_{max}$ in $cm^{-1}$: 3440 (OH), 1662 (C=O), 1625 (C=C). $^1H$ NMR (400 MHz, DMSO-$d_6$): $\delta = 10.47$ (brs, 1H, C-4′-OH), 10.29 (s, 1H, C-2″-OH),

8.02 (m, 3H, H-2′, H-6′, H-3), 7.83 (d, 1H, $J = 15.7$ Hz, H-2), 7.83 (d, 1H, $J = 8.0$ Hz H-3″), 7.25 (t, 1H, $J = 7.6$ Hz, H-5″), 6.88 (m, 4H, H-3′, H-5′, H-4″, H-6″). $^{13}$C NMR (100 MHz, DMSO-$d_6$): $\delta = 187.7$ (C, C-1), 162.2 (C, C-4′), 157.2 (C, C-2″), 138.4 (CH, C-3), 131.9 (CH, C-5″), 131.2 (2CH, C-2′, C-6′), 129.5 (CH, C-3″), 128.7 (C, C-1′), 121.7 (CH, C-2), 121.0 (CH, C-4″), 119.6 (CH, C-6″), 116.3 (C, C-1″), 115.6 (2CH, C-3′, C-5′). HRMS (EI+, 70 eV) *m/z*: 240.0782 for $C_{15}H_{12}O_3$ (calcd. 240.0787).

### (*E*)-1-(4-hydroxyphenyl)-3-(4-methoxyphenyl)-2-propen-1-one (3h)

Yellow crystalline solid, crystallized from EtOH-$H_2O$ (2:3), Yield 50%, mp 82–83 °C. IR (KBr) $\nu_{max}$ in cm$^{-1}$: 3225 (OH), 1650 (C=O), 1602 (C=C). $^1$H NMR (400 MHz, DMSO-$d_6$): $\delta = 10.51$ (1H, brs, C-4′-OH), 8.07 (2H, d, $J =$ 8.6 Hz, H-2′, H-6′), 7.81 (2H, d, $J = 8.52$ Hz, H-2″, H-6″) 7.77 (1H, d, $J = 15.7$ Hz, H-3), 7.67 (1H, d, $J = 15.5$ Hz, H-2), 6.96 (2H, d, $J = 8.6$ Hz, H-3″, H-5″), 6.93 (2H, d, $J =$ 8.6 Hz, H-3′, H-5′), 3.76 (3H, s, C-4″-OMe). $^{13}$C NMR (100 MHz, DMSO-$d_6$): $\delta = 187.4$ (C, C-1), 162.3 (C, C-4′), 161.3 (C, C-4″), 143.0 (CH, C-2), 131.3 (2CH, C-2′, C-6′), 130.7 (2CH, C-2″, C-6″), 129.6 (C, C-1′), 127.7 (C, C-1″), 119.8 (CH, C-3), 115.6 (2CH, C-3′, C-5′), 114.5 (2CH, C-3″ C-5″), 55.4 ($CH_3$, C-4″-OMe). HRMS (EI+, 70 eV) *m/z*: 254.0947 for $C_{16}H_{14}O_3$ (calcd. 254.0943).

### (*E*)-3-(5-chloro-2-hydroxyphenyl)-1-(4-hydroxyphenyl)-2-propen-1-one (3i)

Yellow-orange powder, crystallized from EtOH-$H_2O$ (3:7), Yield 69%, mp 177–178 °C. IR (KBr) $\nu_{max}$ in cm$^{-1}$: 3203 (OH), 1634 (C=O), 1603 (C=C), 757 (C-Cl). $^1$H NMR (400 MHz, DMSO-$d_6$): $\delta = 10.52$ (1H, s, C-4′-OH), 10.45 (1H, s, C-2″-OH), 8.07 (2H, d, $J = 8.4$ Hz, H-2′, H-6′), 8.00 (1H, d, $J = 2.4$ Hz, H-6″), 7.92 (2H, s, H-3, H-2), 7.27 (1H, dd, $J = 2.4$, 8.8 Hz, H-4″), 6.93 (1H, d, $J = 8.8$ Hz, H-3″), 6.89 (2H, d, $J = 8.5$ Hz, H-3′, H-5′). $^{13}$C NMR (100 MHz, DMSO-$d_6$): $\delta = 187.3$ (C, C-1), 162.2 (C, C-4′), 155.8 (C, C-2″), 136.4 (CH, C-3), 131.3 (2CH, C-2′, C-6′), 131.1 (CH, C-4″), 129.3 (C, C-1′), 127.4 (CH, C-6″), 123.4 (C, C-5″), 123.3 (C, C-1″), 122.2 (CH, C-2), 117.9 (CH, C-3″), 115.4 (2CH, C-3′, C-5′). HRMS (EI+, 70 eV) *m/z*: 274.0401 for $C_{15}H_{11}O_3Cl$ (calcd. 274.0397); 276.0388 for $C_{15}H_{11}O_3{}^{37}Cl$ (calcd. 276.0367).

### (*E*)-1,3-bis-(2-hydroxyphenyl)-2-propen-1-one (3j)

Yellow crystalline solid, crystallized from EtOH-$H_2O$ (2:3); Yield: 78%; mp 155–156 °C. IR (KBr) $\nu_{max}$ in cm$^{-1}$: 3406 (OH), 1640 (C=O), 1615 (C=C). $^1$H NMR (400 MHz, DMSO-$d_6$): $\delta = 12.68$ (1H, s, C-2′-OH), 10.42 (1H, s, C-2″-OH), 8.19 (1H, d, $J = 15.1$ Hz, H-3), 8.19 (1H, m, H-6′), 7.98 (1H, d, $J = 15.6$ Hz, H-2), 7.91 (1H, d, $J = 7.6$ Hz, H-3″), 7.55 (1H, t, $J = 7.2$ Hz, H-4′), 7.30 (1H, t, $J = 7.2$ Hz, H-5″), 6.97 (3H, m, H-5′, H-3′, H-6″), 6.89 (1H, t, $J =$ 7.2 Hz, H-4″). $^{13}$C NMR (100 MHz, DMSO-$d_6$): $\delta = 193.9$ (C, Bz-CO), 162.0 (C, C-2′), 157.6 (C, C-2″), 140.4 (CH, C-3), 136.2 (CH, C-4′), 132.6 (CH, C-5″), 130.6 (CH, C-6′), 129.0 (CH, C-3″), 121.0 (C, C-1′), 120.8 (C, C-1″), 120.3 (CH, C-2), 119.5 (CH, C-5′), 119.2 (CH, C-4″), 117.8 (CH, C-3′), 116.4 (CH, C-6″). HRMS (EI+, 70 eV) *m/z*: 240.0778 for $C_{15}H_{12}O_3$ (calcd. 240.0787).

### (*E*)-1-(2-hydroxy-phenyl)-3-(4-methoxyphenyl)-2-propen-1-one (3k)

Yellow powder, crystallized from EtOH-$H_2O$ (1:4); Yield: 77%; mp 85–87 °C. IR (KBr) $\nu_{max}$ in cm$^{-1}$: 2960 ($CH_3$), 1636 (C=O), 1604 (C=C). $^1$H NMR (400 MHz, DMSO-$d_6$): $\delta = 12.78$ (s, 1H, C-2′-OH), 8.25 (d, 1H, $J = 8$ Hz, H-6′), 7.92 (d, 1H, $J = 15.2$ Hz, H-3), 7.88 (d, 2H, $J = 8$ Hz H-2″, H-6″), 7.83 (d, 1H, $J = 15.6$ Hz, H-2), 7.55 (t, 1H, $J = 8$ Hz, H-4′), 7.03 (m, 2H, H-4″, H-5″), 6.99 (m, 2H, H-3′, H-5′), 3.82 (s, 3H, Bz-$OCH_3$). $^{13}$C NMR (100 MHz, DMSO-$d_6$): $\delta = 193.6$ (C, Bz-CO), 162.1 (C, C-2′), 161.8 (C, C-4″), 145.1 (CH, C-2), 136.2 (CH, C-4′), 131.6 (2CH, C-2″, C-6″), 130.8 (CH, C-6′), 127.1 (C, C-1″), 120.6 (C, C-1′0), 119.1 (CH, C-5′), 118.8 (CH, C-3), 117.8 (CH, C-3′), 114.5 (2 CH, C-3″, C-4″), 55.4 ($CH_3$, Bz-OMe). HRMS (EI+, 70 eV) *m/z*: 254.0947 for $C_{16}H_{14}O_3$ (calcd. 254.0943).

### (*E*)-3-(5-chloro-2-hydroxyphenyl)-1-(2-hydroxyphenyl)-2-propen-1-one (3l)

Yellow solid; crystallized from EtOH-$H_2O$ (2:3); Yield 59%; mp 181–183 °C. IR (KBr) $\nu_{max}$ in cm$^{-1}$: 3331 (OH), 1645 (C=O), 1629 (C=C), 748 (C-Cl). $^1$H NMR (400 MHz, DMSO-$d_6$): $\delta = 12.64$ (1H, s, C-2′-OH), 10.70 (1H, s, C-2″-OH), 8.27 (1H, d, $J = 7.6$ Hz, H-6′), 8.2 (1H, d, $J = 15.2$ Hz, H-3), 8.1 (1H, m, H-3″), 8.0 (1H, d, $J =$ 15.2 Hz, H-2), 7.56 (1H, brs, H-4′), 7.31 (1H, d, $J = 7.2$ Hz, H-4″), 6.98 (3H, m, H-3′,H-5′, H-6″). $^{13}$C NMR (100 MHz, DMSO-$d_6$): $\delta = 193.8$ (C, C-1), 162.1 (C, C-2′), 156.3 (C, C-2″), 138.5 (CH, C-3), 136.4 (CH, C-4′), 131.9 (CH, C-5″), 130.9 (CH,C-6′), 127.7 (CH, C-3″), 123.4 (C, C-4″), 122.9 (C, C-1′), 121.5 (CH, C-2), 120.7 (C, C-1″), 119.2 (CH, C-5′), 118.0 (CH, C-6″), 117.8 (CH, C-3′). HRMS (EI+, 70 eV) *m/z*: 274.0390 for $C_{15}H_{11}O_3Cl$ (calcd. 274.0397); 276.0372 for $C_{15}H_{11}O_3{}^{37}Cl$ (calcd. 276.0367).

### (*E*)-1-(2-hydroxy-5-methylphenyl)-3-(2-hydroxyphenyl)-2-propen-1-one (3m)

Pale brown powder, crystallized from EtOH-$H_2O$ (2:3); Yield 37%; mp 122–123 °C. IR (KBr) $\nu_{max}$ in $cm^{-1}$: 3333 (OH), 2924 (CH3), 1636 (C=O), 1604 (C=C). $^1H$ NMR (400 MHz, $CDCl_3$): $\delta = 12.78$ (s, 1H, C-2′-OH), 8.27 (1H, d, $J = 16$ Hz, H-3), 8.27 (1H, d, $J = 16$ Hz, H-3), 7.84 (d, 1H, $J = 16$ Hz, H-2), 7.73 (s, 1H, H-3′), 7.65 (d, 1H, $J = 8$ Hz, H-5′), 7.32 (m, 2H, H-5″, H-6″), 7.0 (m, 2H, H-4″, H-3″), 6.90 (d, 1H, $J = 8$ Hz, H-6′), 2.37 (s, 3H). $^{13}C$ NMR (100 MHz, DMSO-$d_6$): $\delta = 194.6$ (C, C-1), 161.4 (C, C-2′), 155.8 (C, C-2″), 141.0 (CH, C-3), 137.5 (CH, C-4′), 132.1 (CH, C-5″), 129.8 (CH, C-6′), 129.6 (CH, C-3″), 128.0 (C, C-5′), 122.1 (C, C-1′), 121.1 (CH, C-2), 120.9 (C, C-1″), 119.8 (CH, C-4″), 118.3 (CH, C-3′), 116.6 (CH, C-6″), 20.6 (CH3, C-5′-Me). HRMS (EI+, 70 eV) *m/z*: 254.0953 for $C_{16}H_{14}O_3$ (calcd. 254.0943).

### (*E*)-1-(2-hydroxy-5-methyl-phenyl)-3-(4-methoxy-phenyl)-2-propen-1-one (3n)

Yellow oil, purified by preparative TLC (eluent hexane: diethyl ether 8:2), Yield 37%. IR (KBr) $\nu_{max}$ in $cm^{-1}$: 3400 (OH), 2919 (CH3), 1639 (C=O), 1604 (C=C). $^1H$ NMR (400 MHz, DMSO-$d_6$): $\delta = 12.77$ (1H, s, C-2′-OH), 7.90 (1H, d, $J = 14.8$ Hz, H-3), 7.66 (1H, s, H-6′), 7.65 (2H, d, $J = 8.76$ Hz, H-2″, H-6″), 7.55 (1H, d, $J = 15.2$ Hz, H-2), 7.21 (1H, dd, $J = 2$, 8.4Hz, H-4′), 6.96 (2H, d, $J = 8.72$ Hz, H-3″, H-5″), 6.93 (1H, d, $J = 8.48$ Hz, H-3′), 3.87 (3H, s, C-4″-$OCH_3$), 2.36 (3H, s, C-5′-$CH_3$). $^{13}C$ NMR (100 MHz, DMSO-$d_6$): $\delta = 193.8$ (C, C-1), 162.1 (C, C-2′), 161.6 (C, C-4″), 145.3 (CH, C-3), 137.34 (CH, C-4′), 130.7 (2CH, C-2″, C-6″), 129.4 (CH, C-6′), 128.0 (C, C-5′), 127.6 (C, C-1″), 119.9 (C, C-1′), 118.4 (CH, C-3′), 117.9 (CH, C-2), 114.7 (2CH, C-3″, C-5″), 55.6 ($CH_3$, C-4″-OMe), 20.8 ($CH_3$, C-5′-Me). HRMS (EI+, 70 eV) *m/z*: 268.1087 for $C_{17}H_{16}O_3$ (calcd. 268.1100).

### (*E*)-3-(3-chloro-phenyl)-1-(2-hydroxy-5-methyl-phenyl)-2-propen-1- one (3o)

Pale-yellow powder, crystallized from EtOH-$H_2O$ (1:1); Yield 61%; mp 178–179 °C. IR (KBr) $\nu_{max}$ in $cm^{-1}$: 3292 (OH), 1637 (C=O), 1600 (C=C), 753 (C-Cl). $^1H$ NMR (400 MHz, DMSO-$d_6$): $\delta = 12.45$ (1H, s, C-2′-OH), 10.71 (1H, s, C-2″-OH), 8.09 (1H, d, $J = 15.6$ Hz, H-3), 8.05 (2H, s, H-6′, H-6″), 8.01 (1H, d, $J = 15.6$ Hz, H-2), 7.37 (1H, d, $J = 8.4$ Hz, H-4′), 7.32 (1H, d, $J = 8.4$ Hz, H-4″), 6.95 (1H, d, $J = 8.4$ Hz, H-3′), 6.88 (1H, d, $J = 8.4$ Hz, H-3″), 2.31 (3H, s, C-5′-CH3). $^{13}C$ NMR (100 MHz, DMSO-$d_6$): $\delta =$ 193.8 (C, C-1), 160.2 (C, C-2′), 156.3 (C, C-2″), 138.4 (CH, C-3), 137.4 (CH, C-4′), 132.0 (CH, C-4″), 130.5 (CH, C-6′), 128.1 (C, C-5′), 127.6 (CH, C-6″), 123.5 (C, C-5″), 123.0 (C, C-1′), 121.5 (CH, C-2), 120.3 (C, C-1″), 118.1 (CH, C-3′), 117.7 (CH, C-3″), 20.1 ($CH_3$, C-5′-Me). HRMS (EI+, 70 eV) *m/z*: 288.0550 for $C_{16}H_{13}O_3Cl$ (calcd. 288.0553); 290.0525 for $C_{16}H_{13}O_3{}^{37}Cl$ (calcd. 290.0524).

## Antiprotozoal assay

*G. lamblia* strain IMSS:0696:1 was cultured in TYI-S-33 modified medium, supplemented with 10% calf serum (Sigma-Aldrich Co.) and bovine bile (Sigma-Aldrich Co.). For the bioassay (Cedillo-Rivera et al. 2002), the compounds were dissolved in 1 mL of dimethylsulfoxide (DMSO) and added to microtubes containing 1.5 mL of medium to reach concentrations of 0.5, 1.0, 5.0 y 10.0 µg/mL. The solutions were inoculated with *G. lamblia* trophozoites to achieve an inoculum of $4 \times 10^4$ trophozoites/mL and then were incubated for 48 h at 37 °C. Each test included metronidazole as positive control and trophozoites incubated in culture medium with DMSO used in the experiments as the negative control. The used DMSO concentration was not higher than 0.05%. After the incubation, trophozoites were washed and subcultured for another 48 h in fresh medium alone. At the end of this period, trophozoites were counted and the 50% inhibitory concentration ($IC_{50}$) was calculated by Probit analysis. Experiments were carried out in triplicate and repeated at least twice. The level of harmfulness on normal cells was evaluated by determining the selectivity index (SI) of each compound (Vonthron-Sénécheau et al. 2003), which is calculated as the ratio of cytotoxicity on normal cells to antigiardial activity ($SI = IC_{50}$ Vero cells/$IC_{50}$ *G. lamblia*).

## Cytotoxicity assay

Cytotoxicity assay was performed according to the established method of Rahman et al. (2001), where $1.5 \times 10^4$ viable cells, from the Green monkey kidney cell line (Vero cells, ATCC-CCL-81) from the American Type Culture Collection (ATCC), were seeded in a 96-well plate (Costar) and incubated for 24–48 h. When cells reached >80% confluence, the medium was replaced and cells were incubated for 48 h with pure compounds (**3a**–**o**) at 6.25, 12.5, 25, and 50 µg/mL dissolved in DMSO at a maximum concentration of 0.05%. At the end of the exposure time, the medium was removed, and the cells were fixed by adding 50 µL of 10% trichloroacetic acid solution to each well and incubated at 4 °C for 30 min. After incubation, the trichloroacetic acid was eliminated and 50 µL of sulforhodamine B (0.1% sulforhodamine B in 1% acetic acid) were added to each well and left in contact with the cells for 30 min, after which they were washed with 150 µL of 1% acetic acid, and rinsed three times until only dye adhering to

the cells was left. The plates were dried and 100 µL of 10 mM Tris base were added to each well to solubilize the dye. The plates were shaken gently for 10 min and the cellular proliferation was determined by measuring the optical density (OD) at 540 nm using a bioassay reader (BioRad, USA). Docetaxel (Taxotere®; Sigma-Aldrich Co.) was used as positive control, whereas untreated cells were used as a negative control. Each concentration was evaluated by triplicate in an assay by three independent experiments. The cytotoxic activity was calculated as the percentage of cells killed using the equation: growth inhibition (%) = (ODcontrol − ODsample/ODcontrol) × 100. The concentration of pure compounds that killed 50% of the cells ($CC_{50}$) was calculated by GraphPad Prim 4 software.

### Theoretical calculations

The molecular geometries of all compounds were fully optimized using density functional theory with a 6–31G (d, p) basis set. The exchange-correlation potential was evaluated using the hybrid functional B3LYP (Lee et al. 1988). After optimization, a frequencies calculation was performed to characterize all the stationary points at the same computational level and no imaginary frequency was observed. From this calculation, the electrophilicity indexes (ω(eV)) were obtained. All the calculations were carried out using the SPARTAN 16 program. The octanol-water partition coefficients (CLogP) were calculated using the computer program ChemDrawUltra ver. 12.0.2.1076. The ClogP algorithm incorporated in the ChemDraw software is licensed from BioByte Corporation.

The molecular docking studies were performed using the software Autodock v 4.2 and the Autodock tools v 4.2 (ADT) graphical user interface was used to calculate the Gasteiger–Marsili charges for the protein and to add polar hydrogens. The homology model for β-tubulin for *G. intestinalis* was obtained from Guzmán-Ocampo et al. (2018). The polar hydrogen charges of Gasteiger-type were assigned, and the nonpolar hydrogens were merged with the carbon atoms. All the protein was considered as a rigid body and the ligands being flexible. All the torsion and rotatable bonds in the ligand were defined. The grid box for chalcones derivatives were centered at the residue Pheβ200 in the Nocodazole (NZ) site reported in (Aguayo-Ortiz et al. 2013; Guzmán-Ocampo et al. 2018), with a dimension of 80 × 80 × 80 with a spacing grid of 0.375 Å. The search was performed with the Lamarckian Genetic Algorithm as is implemented in Autodock v 4.2 code. The population of 150 individuals was mutated with a mutation rate of 0.02 and envolved for 10 generations. The number of the docking runs was 50. A cluster analysis was performed based on a rms deviation values lower than 2.0 Å referenced to the starting geometry. The best binding mode was selected based on the lowest energy binding and the more populated cluster. The visualization of the complex was done using Maestro (Maestro 2019).

## Results and discussion

A series of 15 chalcones, including a new one (**3i**), showing substitution at rings A and B were synthesized by Claisen–Schmidt condensation with the aid of microwave irradiation (Scheme 1). The yields of the compounds obtained by this procedure ranging from 37 to 78%. All the compounds were characterized by mass spectrometry, $^{1}$H NMR, $^{13}$C NMR, and melting points. The E configuration of the double bond in the structure of the synthesized chalcones was confirmed by the presence in their $^{1}$H NMR spectra of two doublets with high coupling constants ($J$ = 15.1–15.8 Hz).

All synthesized chalcones were evaluated for in vitro antigiardial activity as well as their cytotoxicity against Green monkey kidney cells (Vero cells). The results of the bioassay tests are summarized in Table 1.

The antiprotozoal activity ($IC_{50}$) of five of the chalcones synthesized in this work (**3b**, **3e**, **3h**, **3j**, and **3k**) have been previously reported. Chalcone **3b** exhibited an $IC_{50}$ of 16.25 µM against *G. lamblia*, while it was reported to be active against *Entamoeba histolytica* at 4.76 µM (Wani et al. 2012). The antiplasmodial activity of the compound **3j** has been investigated, finding a moderate $IC_{50}$ of 14.7 µM against *P. falciparum* (Cohen et al. 1998), but in this study, it was resulting in the second more highly antigiardiasic chalcone ($IC_{50}$ = 2.29 µM) with a selectivity index of 20.83. Compound **3k** showed a significant weak activity ($IC_{50}$ = 154.41 µM) against *G. lamblia*, in the same fashion as it has been reported in the literature for its activity against *Trichomonas gallinae* ($IC_{50}$ = 393 µM) (Oyedapo et al. 2004). Chalcones **3e** and **3h** have been previously reported as nonactive compounds against *G. lamblia* (Montes-Avila et al. 2009); similarly, in this study, the antigiardiasic activity detected for these compounds (48.62 and 48.03 µM, respectively) was considered weak.

Sixty percent of 15 synthesized chalcones were considered with significant activity against *G. lamblia*, ranging from 1.3 to 9.35 µM ($IC_{50}$). It is important remark that the activity level of the most active compound against *G. lamblia* (**3m**, $IC_{50}$ 1.03 µM) was slightly better than metronidazole (1.4 µM); additionally, chalcone **3m** resulted in the most selective one (SI = 38.9).

The analysis of the results exhibited in Table 1 revealed that compounds having no substitution at C4″ possess antigiardial activity at IC's$_{50}$ below to 10 µM. The exception to this pattern was chalcone **3f**, which exhibited an $IC_{50}$ of 12.86 µM. It was noteworthy that compounds belonging to

**Scheme 1** Synthetic scheme for the synthesis of chalcones **3a–o**

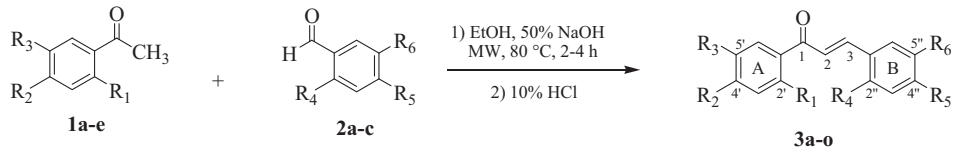


**1a-e**

| | $R_1$ | $R_2$ | $R_3$ |
|---|---|---|---|
| **1a** | H | Me | H |
| **1b** | H | OMe | H |
| **1c** | H | OH | H |
| **1d** | OH | H | H |
| **1e** | OH | H | Me |

**2a-c**

| | $R_4$ | $R_5$ | $R_6$ |
|---|---|---|---|
| **2a** | OH | H | H |
| **2b** | H | OMe | H |
| **2c** | OH | H | Cl |

**3a-o**

**Table 1** Antigiardial activity, selectivity index, electrophilicity, and lipophilicity of synthesized chalcones

| Comp | Substituent position | | | | | | *G. lamblia* | Vero Cells | SI[b] | CLogP[c] | ω(eV)[d] |
|---|---|---|---|---|---|---|---|---|---|---|---|
| | 2′ | 4′ | 5′ | 2″ | 4″ | 5″ | $IC_{50}$ μM ± SD[a] | $CC_{50}$ μM ± SD | | | |
| **3**[a] | H | Me | H | OH | H | H | 6.48 ± 1.55 | 25.83 ± 1.29 | 3.99 | 3.46 | 1.86 |
| **3b** | H | Me | H | H | MeO | H | 16.25 ± 1.19 | 49.96 ± 1.35 | 3.08 | 4.04 | 1.63 |
| **3c** | H | Me | H | OH | H | Cl | 5.98 ± 1.11 | 22.52 ± 1.29 | 3.76 | 4.47 | 2.01 |
| **3d** | H | MeO | H | OH | H | H | 9.35 ± 1.41 | 46.26 ± 1.02 | 4.95 | 3.18 | 1.80 |
| **3e** | H | MeO | H | H | MeO | H | 48.62 ± 1.22 | 61.57 ± 1.20 | 1.27 | 3.73 | 1.57 |
| **3f** | H | MeO | H | OH | H | Cl | 12.86 ± 1.03 | 32.36 ± 1.20 | 2.52 | 4.19 | 1.95 |
| **3g** | H | OH | H | OH | H | H | 5.34 ± 1.37 | 42.63 ± 1.33 | 7.98 | 2.83 | 1.81 |
| **3h** | H | OH | H | H | MeO | H | 48.03 ± 1.10 | 79.61 ± 1.18 | 1.66 | 3.42 | 1.60 |
| **3i** | H | OH | H | OH | H | Cl | 3.60 ± 1.04 | 23.07 ± 1.39 | 6.40 | 3.84 | 1.97 |
| **3j** | HO | H | H | OH | H | H | 2.29 ± 1.22 | 47.67 ± 1.04 | 20.83 | 3.29 | 1.54 |
| **3k** | HO | H | H | H | MeO | H | 154.41 ± 1.16 | 63.90 ± 1.22 | 0.41 | 3.88 | 1.55 |
| **3l** | HO | H | H | OH | H | Cl | 3.47 ± 1.15 | 21.22 ± 1.35 | 6.12 | 4.30 | 1.88 |
| **3m** | HO | H | Me | OH | H | H | 1.03 ± 1.13 | 39.92 ± 1.08 | 38.91 | 3.79 | 1.69 |
| **3n** | HO | H | Me | H | MeO | H | 40.93 ± 1.45 | 56.40 ± 1.19 | 1.38 | 4.38 | 1.53 |
| **3o** | HO | H | Me | OH | H | Cl | 2.20 ± 1.24 | 10.73 ± 1.36 | 4.87 | 4.80 | 1.89 |
| **Metronidazole** | | | | | | | 1.40 | | | | |
| **Docetaxel** | | | | | | | | 1.30 | | | |

[a]Standard deviation

[b]Selectivity index

[c]Logarithm of calculated octanol-water partition coefficient

[d]Electrophylicity index

this set having hydroxyl substituents at carbons 2′ and 2″, as well as a methyl group at carbon 5′, exhibit the lowest inhibitory concentrations against *G. lamblia* (**3m** and **3o**). Also, it was observed a slight decreasing in the bioactivity of their analogs without substituents at C5′ (**3j** and **3l**).

In addition, if the set of ten compounds above mentioned is divided into two subgroups, based on the substituent presents at C5″, it is possible to observe that the presence of a chlorine atom, in general, provokes a decreasing of the antigiardial activity. This effect was more pronounced over the selectivity of the most active compounds, thereby chalcone **3o** was eightfold less selective than chalcone **3m**, and the selectivity of **3l** decreased 3.4 times compared to that of **3j**.

It is interesting to note that the presence of a methoxyl group at C4′ or C4″ together with the absence of substituents at C2″ cause a dramatic negative effect on the activity against *G. intestinalis*. Thereby, chalcones **3e**, **3h** and **3n** were at least 40-fold less active than the most active one while chalcone **3k** was the less active compound ($IC_{50} = 154$ μM).

The broad spectrum of biological activity of chalcones, including antiprotozoal activity, has been attributed, mainly, to their Michael acceptor features (Gaonkar and Vignesh 2017; Gomes et al. 2017; Zhuang et al. 2017); therefore, the electrophilicity of the enone moiety may play an important role in the mechanisms of action of this class of compounds. In addition, the increase of lipophilicity has been also

associated with an increase in the antigiardiasic activity of some compounds (Mocelo-Castell et al. 2015).

To explore the SAR relationships of synthesized chalcones, their octanol-water partition coefficients (CLogP) and electrophilicity indexes were calculated (Table 1).

The CLogP's ranging from 2.83 to 4.80. Noteworthy, the calculated partition coefficients for the most active (**3m**) and the less active (**3k**) chalcones (3.79 and 3.88, respectively) exhibited a non-significant difference. Moreover, the antigiardiasic activity and CLogP (Table 1) of the four most active compounds (**3j**, **3l**, **3m**, and **3o**) exhibited a slight inverse proportional relationship, thus the most active chalcones **3m** and **3j** ($IC_{50} = 1.03$ and 2.20 μM, respectively) were less lipophilic than their respective chlorine analogs **3o** and **3l** ($IC_{50} = 2.29$ and 3.47 μM, respectively). Contrary to our expectations, the relationship pattern exhibited by the four most active chalcones was not observed for the complete set of synthesized chalcones, indeed it was not possible to find some correlation between their ClogP's and antiprotozoal activity. Then, the SAR analysis was expanded adding the antigiardial activity ($IC_{50}$'s = 49.69, 55.29, and 63.79 μM) and CLogP's (3.62, 4.02, and 4.23) of three previously reported chalcones **C1**, **C2** and **C3**, respectively (Fig. 1) (Montes-Avila et al. 2009). Noteworthy, the slight inverse correlation was observed again. It is important remark that chalcones **C1**, **C2** and **C3** present chlorine or fluorine atoms as substituents, thus the weak inverse correlation could be associated with the presence of halogens in chalcones' structure.

As it can see in Table 1, the electrophilicity indexes of chalcones with significant activity present a modest inverse correlation with the antiprotozoal activity. On the other hand, the chalcones with values of $IC_{50}$ higher than 10 μM exhibited a slight direct relationship. Therefore, in the same fashion of the calculated octanol-water partition coefficients, the electrophilicity indexes of the previously reported chalcones **C1**, **C2** and **C3** (1.97, 2.12, and 2.08, respectively) were added to SAR analysis. Unfortunately, the inclusion of the data mentioned above provokes the loss of both observed trending. This contrasting behavior not allowed to determine a clear correlation between antiprotozoal activity and the electrophilicity of the studied chalcones.

Interestingly, although the Michael acceptor mechanism is known as the representative mechanism of action of chalcones, the obtained results suggest that antigiardial activity exhibited for synthesized chalcones is not due to it. Fortunately, tremendous efforts devoted to characterizing the mechanisms of chalcones activity have resulted in the identification of new therapeutic targets, like inhibition of receptor tyrosine kinase, cyclooxygenase, and aldose reductase activities, as well as the inhibition of microtubules formation (Zhuang et al. 2017).

It is known that the binding of microtubule target agents at the colchicine site of tubulin can disrupt the formation of microtubules. Colchicine site is a domain divided into three zones: The zone 1 is found at the α unit of the interface, zone 2 is located at β subunit, while zone 3 is buried deeper in the β subunit (Li et al. 2017).

The affinity of chalcones to binding to the colchicine site has been determined using a 5D-QSAR model for combretastatin-like analogs (Ducki et al. 2005) due to similarity between combretastatin A4 (CA-4) and this class of compounds. CA-4 belongs to colchicine binding site inhibitors (CBSIs) which have globular o butterfly shape that allows them can accommodate into the binding pocket at zones 1 and 2 (Pérez-Pérez et al. 2016).

Previous to molecular docking, the molecular geometries of compounds to be docked were fully optimized. Surprisingly, some low-energy conformers of each compound exhibited an almost planar shape instead of the expected butterfly shape. It is important to remark that this shape is similar to that exhibited for benzimidazoles, one of the classes of the drugs available for the treatment of giardiasis (Fennell et al. 2008), when they are bonded to colchicine site (Li et al. 2017).

Benzimidazoles (nonclassical CBSIs) bind to the colchicine motif at zone 3 and also present a little overlapping with zone 2 (Li et al. 2017). This feature, together with the fact the homology model for *Giardia* β-tubulin only describes the peptide sequence of zone 3 (Aguayo et al. 2013, 2), made it reasonable to perform docking of the synthesized chalcones into zone 3 of the colchicine domain.

A molecular docking study of four most active chalcones (**3m**, **3o**, **3j**, and **3l**) was performed using a homology model for *Giardia* β-tubulin as a target receptor, taken from Guzmán-Ocampo et al. (2018). Remarkably, binding affinity values of docked compounds ranged from −7.52 to −6.88 kcal/mol, resulting very close to the docking score obtained for the binding of Nocodonazole (NZ) with colchicine site (−8.05 kcal/mol). Noteworthy, it has been reported that NZ is active against *G. lamblia* at an $IC_{50}$ of 0.017 μM (Katiyar et al. 1984) and its binding energy is −9.10 kcal/mol (Aguayo-Ortiz et al. 2013).

The binding site pocket for NZ in homology model for *Giardia* β-tubulin consists of Tyr50, Gln134, Cys165, Phe167, Glu198, Phe200, Thr237 Cys239, Leu240, Leu250, Leu253, Leu257, and Phe266; among them, Glu98 has special importance due it plays a determinant role in the stabilization of ligands through the formation of two hydrogen bonds. After its formation, this interaction can be reinforced by the establishment of interactions with Cys135 and Cys239 (Aguayo-Ortiz et al. 2013).

Surprisingly, in our docking study, it was found that the four chalcones (**3m**, **3o**, **3j**, and **3l**) established hydrogen bonds between carbonyl group of enone system and Glu98 residue (Fig. 2), as it has been determined for NZ. The

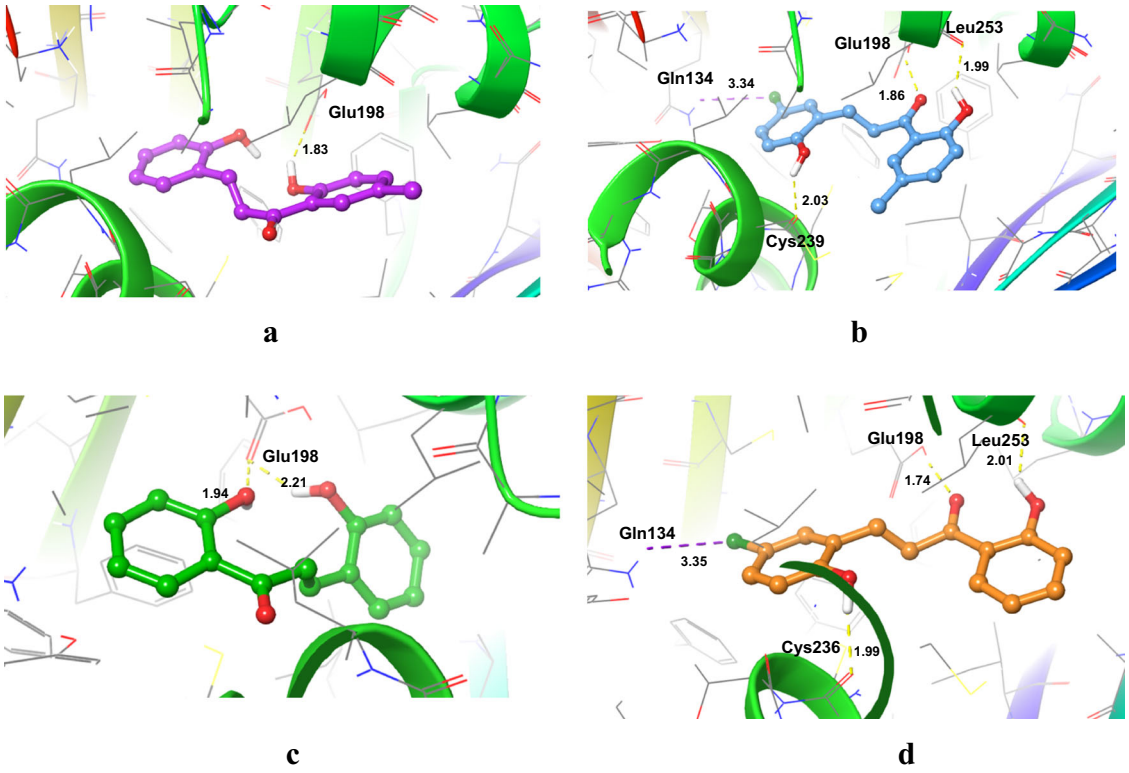


**Fig. 2** Docking images of four most active chalcones binding colchicine site of homology model for *Giardia* β-tubulin. **a** Compound **3m**. **b** Compound **3o**. **c** Compound **3j**. **d** Compound **3k**

H-bond distances for chalcones ranged between 1.74 and 2.21 Å, while NZ exhibited distances of 1.71 and 2.35 Å. Moreover, compound **3o** was capable to interact with Cys239 through another hydrogen bond. Thus, it could support that the antigiardial activity exhibited by the synthesized chalcones is due to their binding affinity toward the zone 3 of the colchicine site of *Giardia* β-tubulin (Fig. 3).

Moreover, the hydrogen bond formed between the oxygen atom of the enone carbonyl group and Glu198 residue probably increases the electrophilicity of the enone β carbon. However, significantly, the docking study did not show any interaction between the enone system carbons of studied chalcones and the amino acid residues of zone 3 of the colchicine site.

This fact, together with the unclear relationship between the electrophilicity indexes of chalcones and their antiprotozoal activity, allows speculating that the action mechanism of antigiardial activity may not follow the Michael acceptor mechanism.

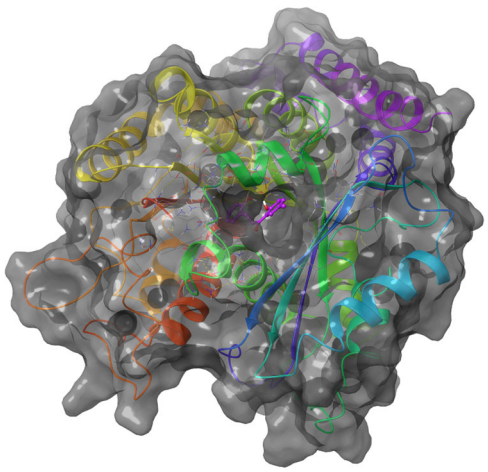

**Fig. 3** Compound **3m** docked at zone 3 of the colchicine site of the homology model of *Giarda* β-tubulin

## Conclusions

In summary, a total of 15 chalcones with different substituents at rings A and B were synthesized by microwave-assisted Claisen–Schmidt condensation, fully characterized by NMR and MS spectra, and tested against the pathogenic intestinal protozoan *Giardia lamblia*, and Vero cells.

To the best of our knowledge, the (*E*)-3-(5-chloro-2-hydroxyphenyl)-1-(4-hydroxyphenyl)-2-propen-1-one (**3i**, $IC_{50} = 3.60\ \mu M$) has not previous reports in the literature.

Nine chalcones were active against *G. lamblia* at $CI_{50} < 10\ \mu M$, among them, five exhibited $CI_{50}$ values lower than

5 μM. The chalcone **3m** was the most active compound with an $IC_{50}$ of 1.03 μM and the highest selective one (SI = 38.9). It is important to note that, the antigiardial activity of this compound was better than that showed by metronidazol ($CI_{50} = 1.4$ μM). The structure relationship analysis suggests that: (i) electro-donating groups at 2′, 2″ and 5′ positions enhanced the antigiardial activity, (ii) the presence of chlorine at C5″ negatively affects the selectivity, (iii) the electrophilicity of the most active chalcones presents a slight inverse correlation with the antigiardial activity. The docking study results allow supposing that antigiardial chalcones bind to colchicine site at zone 3 and speculate that their action mechanism does not follow the Michael acceptor mechanism.

Finally, our findings encourage us to synthesize a series of chalcones with electron-donating groups at 2′, 2″ and 5′ positions to perform a QSAR for their antigiardial activity.

**Acknowledgements** Funding for this research was provided by Facultad de Química, Universidad Autónoma de Yucatan. The docking analysis was performed as part of the research project 256657 granted by the Consejo Nacional de Ciencia y Tecnología - México (CONACYT). In memory of Dr. José Antonio Manzanilla Cano (1964-2015), for his invaluable support.

## Compliance with ethical standards

**Conflict of interest** The authors declare that they have no conflict of interest.

**Publisher's note** Springer Nature remains neutral with regard to jurisdictional claims in published maps and institutional affiliations.

## References

Aguayo-Ortiz R, Méndez-Lucio O, Romo-Mancillas A, Castillo R, Yépez-Mulia L, Medina-Franco JL, Hernández-Campos A (2013) Molecular basis for benzimidazole resistance from a novel β-tubulin binding site model. J Mol Graph Model 45:26–37

Ankarklev J, Jerlström-Hultqvist J, Ringqvist E, Troell K, Svärd SG (2010) Behind the smile: cell biology and disease mechanisms of Giardia species. Nat Rev Microbiol 8:413–422

Cedillo-Rivera R, Chavez B, Gonzalez-Robles A, Tapia A, Yepez-Mulia L (2002) Physiology and ecology-in vitro effect of nitazoxanide against *Entamoeba histolytica*, Giardia intestinalis and Trichomonas vaginalis trophozoites. J Eukaryot Microbiol 49:201–208

Cohen FE, McKerrow JH, Kenyon GL, Li Z, Chen X, Gong B, Li R (1998) Inhibitors of metazoan parasite proteases. US Patent 1998-5739170, filled 30 Mar 1995, issued 14 Apr 1998

Ducki S, Mackenzie G, Lawrence NJ, Snyder JP (2005) Quantitative structure-activity relationship (5D-QSAR) study of combretastatin-like analogues as inhibitors of tubulin assembly. J Med Chem 48:457–465

Escobedo A, Almirall P, Robertson LJ, Franco RMB, Hanevik K, Morch K, Cimerman S (2010) Giardiasis: The ever-present threat of a neglected disease. Infect Disord Drug Targ 10:329–348

Fennell BJ, Naughton JA, Barlow J, Brennan G, Fairweather I, Hoey E, McFerran N, Trudgett A, Bell A (2008) Microtubules as antiparasitic drug targets. Expert Opin Drug Discov 3:501–518

Gaonkar SL, Vignesh UN (2017) Synthesis and pharmacological properties of chalcones: a review. Res Chem Intermed 43:6043–6077

Gomes M, Muratov E, Pereira M, Peixoto J, Rosseto L, Cravo P, Andrade C, Neves B (2017) Chalcone derivatives: promising starting points for drug design. Molecules 22:1210–1235

Guzmán-Ocampo DC, Aguayo-Ortiz R, Cano-González L, Castillo R, Hernández-Campos A, Dominguez L (2018) Effects of the protonation state of titratable residues and the presence of water molecules on nocodazole binding to β-tubulin. ChemMedChem 13:20–24

Halliez MC, Buret AG (2013) Extra-intestinal and long term consequences of Giardia duodenalis infections. World J Gastroenterol 19:8974–8985

Katiyar SK, Gordon VR, Mclaughlin GL, Edlind TD (1984) Antiprotozoal activities of benzimidazoles and correlations with β-tubulin sequence. Antimicrob Agents Chemother 38:2086–2090

Lee C, Yang W, Parr RG (1988) Development of the Colle-Salvetti correlation-energy formula into a functional of the electron density. Phys Rev B 37:785–789

Li W, Sun H, Xu S, Zhu Z, Xu J (2017) Tubulin inhibitors targeting the colchicine binding site: a perspective of privileged structures. Future Med Chem 9:1765–1794

Maestro, Schrödinger, LLC, New York, NY, 2019

Mocelo-Castell R, Villanueva-Novelo C, Cáceres-Castillo D, Carballo RM, Quijano-Quiñones RF, Quesadas-Rojas M, Cantillo-Ciau Z, Cedillo-Rivera R, Moo-Puc RE, Moujir LM, Mena-Rejón GJ (2015) 2-Amino-4-arylthiazole derivatives as anti-giardial agents: synthesis, biological evaluation and QSAR studies. Open Chem 13:1127–1136

Montes-Avila J, Díaz-Camacho SP, Sicairos-Félix J, Delgado-Vargas F, Rivero IA (2009) Solution-phase parallel synthesis of substituted chalcones and their antiparasitary activity against Giardia lamblia. Bioorg Med Chem 17:6780–6785

Pasupuleti V, Escobedo AA, Deshpande A, Thota P, Roman Y, Hernandez AV (2014) Efficacy of 5-nitroimidazoles for the treatment of giardiasis: a systematic review of randomized controlled trials. Plos Negl Trop Dis 8:e2733

Pérez-Pérez M-J, Priego E-M, Bueno O, Martins MS, Canela M-D, Liekens S (2016) Blocking blood flow to solid tumors by destabilizing tubulin: an approach to targeting tumor growth. J Med Chem 59:8685–8711

Pires SM, Fischer-Walker CL, Lanata CF, Devleesschauwer B, Hall AJ, Kirk MD, Duarte ASR, Black RE, Angulo FJ (2015) Aetiology-specific estimates of the global and regional incidence and mortality of diarrhoeal diseases commonly transmitted through food. PLoS ONE 10:e0142927

Oyedapo AO, Makanju VO, Adewunmi CO, Iwalewa EO, Adenowo TK (2004) Antitrichomonal activity of 1,3-diaryl-2-propen-1-ones on *Trichomonas gallinae*. Afr J Trad CAM 1:55–62

Rahman A, Choudhary MI, Thomsen WJ (2001) Bioassay techniques for drug development. Harwood Academic Publishers, Netherlands

Sahu NK, Balbhadra SS, Choudhary J, Kohli DV (2012) Exploring pharmacological significance of chalcone scaffold: a review. Curr Med Chem 19:209–225

Savioli L, Smith H, Thompson A (2006) Giardia and Cryptosporidium join the neglected diseases initiative'. Trends Parasitol 22:203–208

Thompson RCA (2000) Giardiasis as a re-emerging infectious disease and its zoonotic potential. Int J Parasitol 30:1259–1267

Upcroft P, Upcroft JA (2001) Drug targets and mechanisms of resistance in the anaerobic protozoa. Clin Microbiol Rev 14:150–164

Vonthron-Sénécheau C, Bernard-Weniger B, Ouattara M, Tra-Bi F, Kamenan A, Lobstein A, Brun R, Anton R (2003) In vitro antiplasmodial activity and cytotoxicity of ethnobotanically selected Ivorian plants. J Ethnopharmacol 87:221–222

Wani MY, Bhat AR, Azam A, Lee DH, Choi I, Athar F (2012) Synthesis and in vitro evaluation of novel tetrazole embedded 1,3,5-trisubstituted pyrazoline derivatives as *Entamoeba histolytica* growth inhibitors. Eur J Med Chem 54:845–854

Zhuang C, Zhang W, Sheng C, Zhang W, Xing C, Miao Z (2017) Chalcone: a privileged structure in medicinal chemistry. Chem Rev 117:7762–7810